Journal of Zhejiang University-SCIENCE C (Computers & Electronics)
ISSN 1869-1951 (Print); ISSN 1869-196X (Online)
www.zju.edu.cn/jzus; www.springerlink.com
E-mail: jzus@zju.edu.cn

New method for estimating flying capacitor voltages in stacked multicell and flying capacitor multicell converters

Arash KHOSHKBAR SADIGH[†1], Gevorg B. GHAREHPETIAN[2], Seyed Hossein HOSSEINI[1]

([1]*Faculty of Electrical & Computer Engineering, University of Tabriz, Tabriz 51666, Iran*)

([2]*Department of Electrical Engineering, Amirkabir University of Technology, Tehran 15914, Iran*)

[†]E-mail: a.khoshkbar.sadigh@ieee.org

Received Sept. 10, 2009; Revision accepted Jan. 5, 2010; Crosschecked July 1, 2010

Abstract: Multicell converters are an interesting alternative for medium voltage and high power applications, because of the increased number of output voltage levels and apparent frequency. The two most significant types of multicell converter are the flying capacitor multicell (FCM) converter and its derivative, stacked multicell (SM) converter. Balancing flying capacitor voltages is an important constraint to the proper performance of FCM and SM converters. Thus, observation of the flying capacitor voltages used in active control is valuable, but using voltage sensors for observation increases cost and size of the converter. This paper deals with a new strategy to estimate the flying capacitor voltages of both FCM and SM converters. The proposed strategy is based on a discrete time model of the converter and uses only a load current sensor. The circuit was simulated using PSCAD/EMTDC software and simulation results were presented to validate the effectiveness of the proposed estimation strategy in observing the flying capacitor voltages. Simplicity is the most significant advantage of the proposed strategy, its performance being based on simple equations.

Key words: Flying capacitor multicell converter, Stacked multicell converter, Flying capacitor voltage, Phase shifted sinusoidal pulse width modulation

doi:10.1631/jzus.C0910559 **Document code:** A **CLC number:** TM464

1 Introduction

Multicell converters have been continuously developed in recent years due to the need for an increased power level in industry, especially for high power applications such as high power motor drives, active power filters, reactive compensation, flexible AC transmission systems (FACTS) devices, and distributed generation (Hu and He, 2007; Hu *et al.*, 2007; Sayyah *et al.*, 2008; Halvaei Niasar *et al.*, 2009; Li *et al.*, 2009). These have the capability of handling voltage in the range of kilovolts and power of several megawatts, especially with recent developments in the area of high power semiconductors (Turpin *et al.*, 2002; Haederli *et al.*, 2006; Lezana *et al.*, 2007; 2008b; Ma and He, 2008).

© Zhejiang University and Springer-Verlag Berlin Heidelberg 2010

Multicell converters include an array of power semiconductors and flying capacitors, with their desired operating voltage, which generate an output voltage with stepped waveforms. The commutation of the switches permits the addition of the flying capacitor voltages and generates high voltage at the output while the power semiconductors encounter only reduced voltages (Babaei *et al.*, 2007; Lezana *et al.*, 2008a; McGrath and Holmes, 2008).

The term ‘multilevel’ comes from the three-level converter introduced by Nabae *et al.* (1981). By increasing the number of levels in the converter, the output voltage has more steps, generating a staircase waveform which has a reduced harmonic distortion (Meynard *et al.*, 1997). The neutral point clamped (NPC) converter presented in Nabae *et al.* (1981) is now a standard topology in industry in its three-level version. For a high number of levels, however, this topology presents some problems, mainly with the clamping diodes and the balance of the dc-link capacitors. An alternative for the NPC converter is the multicell topologies. Different cells and ways to interconnect them generate many topologies, among which the most important ones are the cascaded multicell (CM) and the flying capacitor multicell (FCM) with its sub-topology stacked multicell (SM) converters (Meynard *et al.*, 2002; Babaei *et al.*, 2007; Khoshkbar Sadigh *et al.*, 2009a; 2009b; 2009c).

The FCM converter (Meynard *et al.*, 2006) and its derivative, the SM converter (Lienhardt *et al.*, 2007), have many attractive properties for medium voltage applications including in particular the advantage of transformerless operation and the ability to naturally maintain the flying capacitor voltages at their target operating levels (Meynard *et al.*, 2006; Lienhardt *et al.*, 2007; McGrath *et al.*, 2007). This important property is called natural balancing and allows the construction of converters with a large number of voltage levels.

The balancing of the flying capacitor voltages guarantees the suitable performance of FCM and SM converters and determines the lifetime of these converters (Hosseini *et al.*, 2009). Thus, having knowledge of flying capacitor voltages is valuable and it is important in the active control of the FCM and SM converters (Lienhardt *et al.*, 2007). Measuring their quantities by voltage sensors, however, is difficult and expensive due to the voltage levels and increases the size and cost of the converter (Ruelland *et al.*, 2003; Lienhardt *et al.*, 2006a; 2006b; 2007; Hosseini *et al.*, 2009). For this reason, a simple and effective estimation strategy is substantial, essential, and useful for observing the flying capacitor voltages. In this paper, a simple estimation strategy based on a discrete time model of the FCM and SM converters is proposed which requires only the sensing of the load current.

2 Reminder on the flying capacitor multicell converter

The FCM converter uses a series connection of 'cells' comprising a flying capacitor and its associated complimentary switch pair and produces a stepped voltage that is the sum of the individual cell voltages (McGrath *et al.*, 2007; McGrath and Holmes, 2008). An n-cell FCM converter (Fig. 1) is composed of $2n$ switches forming n-commutation cells controlled with equal duty cycles, $n-1$ flying capacitors with the same capacitance and different dc rating voltages equal to E/n, $2E/n$, …, $(n-1)E/n$. As a result, the electrical stress on each switch is reduced and more equally distributed as each switch must support a voltage of E/n (Meynard *et al.*, 2006).

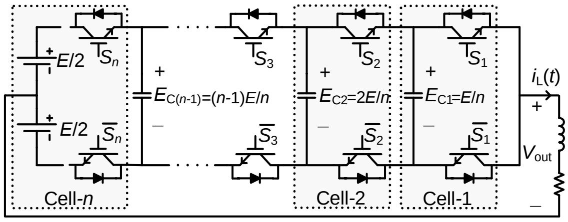

Fig. 1 An *n*-cell flying capacitor multicell converter

As mentioned, the self-balancing property is one of the important advantages of the FCM converter (Meynard *et al.*, 2002; 2006; Lienhardt *et al.*, 2007; McGrath *et al.*, 2007; Khoshkbar Sadigh *et al.*, 2009a; 2009b; 2009c). The natural self-balancing of the flying capacitors occurs without any feedback control. A necessary self-balancing condition is that the average flying capacitor current must be zero. As a result, each cell must be controlled with the same duty cycle and a regular phase shifted sinusoidal pulse width modulation (PS-SPWM) progression along the cells. As shown in Fig. 2, a 4-cell-5-level FCM converter is controlled by a regular PS-SPWM where the phase shift between the carriers of each cell is (Turpin *et al.*, 2002; Hosseini *et al.*, 2009; Khoshkbar Sadigh *et al.*, 2009a)

$$\phi = 2\pi / n, \tag{1}$$

where n is the number of the cells that work in each half cycle and equals 4 in the 4-cell-5-level FCM converter. The switch states of the 4-cell-5-level FCM converter are demonstrated in Table 1.

In general, an output RLC filter (for balancing booster circuit), tuned to the switching frequency, has to be connected across the load to accelerate the self-balancing process in the transient states and to reduce the effect of control signal faults (Turpin *et al.*, 2002). In this case, the dynamic of the transient depends on the impedance of load at the switching frequency. If the impedance at the switching frequency is high (small current harmonic at this frequency) then the natural balancing is very slow, and vice versa. The output RLC filter is tuned to the switching frequency as follows:

$$\sqrt{LC} = f_{\mathrm{SW}} / (2\pi), \tag{2}$$

where f_{SW} is the switching frequency, and L and C are inductance and capacitance of the output RLC filter, respectively.

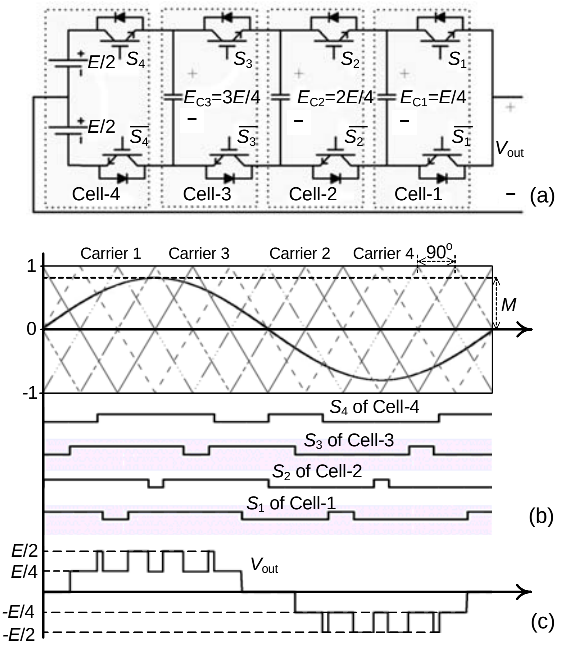

Fig. 2 Four-cell-five-level flying capacitor multicell converter's control strategy (a), switch states (b), and output voltage (c)

Table 1 States of switches in the 4-cell-5-level flying capacitor multicell converter

Output voltage level	State(s) of (S_4, S_3, S_2, S_1)	Number of states
$+2E/4$	(1, 1, 1, 1)	1
$+E/4$	(1, 1, 1, 0), (1, 1, 0, 1), (1, 0, 1, 1), (0, 1, 1, 1)	4
0	(1, 1, 0, 0), (1, 0, 0, 1), (0, 0, 1, 1), (0, 1, 1, 0)	4
$-E/4$	(0, 0, 0, 1), (0, 0, 1, 0), (0, 1, 0, 0), (1, 0, 0, 0)	4
$-2E/4$	(0, 0, 0, 0)	1

3 Reminder on the stacked multicell converter

An alternative topology based on the FCM converter is the SM converter, which stacks two FCM converters together: the upper stack is switched only when a positive output is required, and the lower stack is switched only when a negative output is required (Lienhardt *et al.*, 2007; McGrath *et al.*, 2007; Hosseini *et al.*, 2009). The SM converter structure uses an $m\times n$ cell array to increase the number of output voltage levels.

A 2n-cell SM converter is shown in Fig. 3. The main advantages of this configuration are that the number of combinations to obtain a desired voltage level is increased and the voltage ratings of capacitors and stored energy in the flying capacitors as well as the semiconductor losses are reduced (Meynard *et al.*, 2006; Lienhardt *et al.*, 2007; McGrath *et al.*, 2007; Hosseini *et al.*, 2009). It requires, however, the same number of capacitors and semiconductors in comparison with the equivalent FCM converter for the same number of output voltage levels (Khoshkbar Sadigh *et al.*, 2009a).

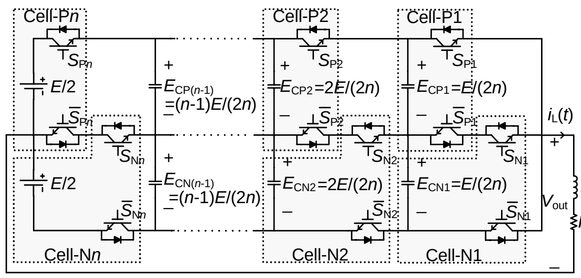

Fig. 3 A 2n-cell stacked multicell converter

A 2n-cell SM converter (Fig. 3) is composed of 4n switches forming 2n-commutation cells controlled with equal duty cycles, $2n-2$ flying capacitors with the same capacitance and different dc rating voltages equal to $E/(2n)$, $2E/(2n)$, …, $(n-1)E/(2n)$. As a result, the electrical stress on each switch is reduced and more equally distributed as each switch must support a voltage of $E/(2n)$ (Khoshkbar Sadigh *et al.*, 2009a).

Like the FCM converter, the 4-cell-5-level SM converter (Fig. 4) is controlled by a regular PS-SPWM, where the phase shift between the carriers of each cell is as shown by Eq. (1), with n being the number of the cells that work in each half cycle. n equals 2 in the 4-cell-5-level SM converter. The switch states of the 4-cell-5-level SM converter are given in Table 2. Like the FCM converter, the SM converter has the self-balancing property and each cell must be controlled with the same duty cycle and a regular phase shifted progression along the cells (Meynard *et al.*, 2002; Lienhardt *et al.*, 2007; Khoshkbar Sadigh *et al.*, 2009a).

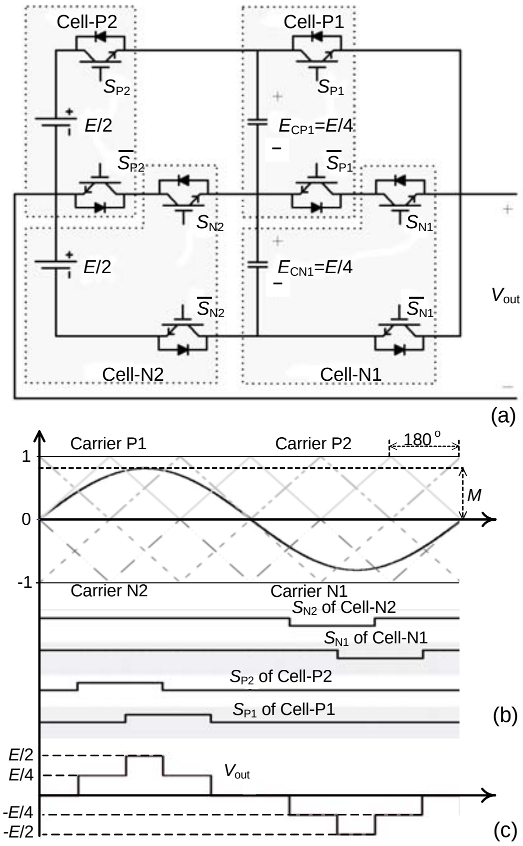

Fig. 4 Four-cell-five-level stacked multicell converter's control strategy (a), switch states (b), and output voltage (c)

Table 2 States of switches in the 4-cell-5-level stacked multicell converter

Output voltage level	State(s) of switches $\{(S_{P2}, S_{P1}), (S_{N2}, S_{N1})\}$	Number of states
$+2E/4$	{(1, 1), (1, 1)}	1
$+E/4$	{(1, 0), (1, 1)}, {(0, 1), (1, 1)}	2
0	{(0, 0), (1, 1)}, {(1, 0), (1, 0)}, {(0, 1), (0, 1)}	3
$-E/4$	{(0, 0), (1, 0)}, {(0, 0), (0, 1)}	2
$-2E/4$	{(0, 0), (0, 0)}	1

4 Estimation of flying capacitor voltages

As reported in Turpin *et al.* (2002) and Hosseini *et al.* (2009), an active control of the FCM and SM converters requires the knowledge of the states, especially the flying capacitor voltages. Usually, differential voltage sensors are used to measure the flying capacitor voltages, but the presence of these sensors increases the drive cost and size. As an example, the active control of a 3-cell 3-phase FCM converter or a 4-cell 3-phase SM converter requires at least 6 floating voltage sensors. Furthermore, in medium voltage applications, the design of the voltage sensors is not simple and usually requires a good insulation quality (Turpin *et al.*, 2002; Hosseini *et al.*, 2009).

To reduce the number of sensors, several solutions are available and have been tested. The simplest one needs only one voltage sensor. Its basic principle consists of the measurement of the converter output voltage each time the input control vector changes. Thus, using switch states information, one can easily obtain the capacitors and supply voltages by resolving a linear algebraic equation of the system. Obviously, this method does not correspond to a state observation since the system dynamics are not considered.

The major drawback of the aforementioned estimation techniques is the high measurement noise sensitivity, since any perturbation on the measurement is directly transposed to the estimated states. Moreover, in those techniques one voltage sensor is also required.

The other solution is to develop a state observer using a load current measurement. For this purpose, a good model representation of the system must be adopted. A sliding mode observation technique based on using a load current measurement has been proposed (Lienhardt *et al.*, 2006a; 2006b; 2007). In the sliding mode observation technique as discussed in Lienhardt *et al.* (2006a; 2006b; 2007), there are some disadvantages as follows:

1. Many coefficients in the model of the converter must be calculated, and these depend on the system parameters such as load characteristic and flying capacitor voltages. As a result, a complex model of the converter is achieved. Meanwhile, some of these coefficients must be guessed.

2. The observer gain matrix, $\boldsymbol{\Lambda}$, must be calcu-

lated according to the assumed maximum error of estimated flying capacitor voltages and load current. In this case, the maximum load current must be definite. Thus, this matrix must be calculated for each case, which makes the technique time consuming.

3. The saturation function as well as the correction functions must be implemented, which increases the number of calculations and the complexity of the technique.

4. In addition to the calculation of flying capacitor voltages, it is essential to calculate the load current for use in the saturation function and correction functions, which leads to an increased number of calculations and the complexity of the technique.

To overcome these problems, we study and describe an exact discrete time model of the converter for estimating the flying capacitor voltages of a 4-cell-5-level FCM converter as well as SM converter. Modeling of FCM and SM converters is expressed in the following parts.

4.1 Modeling of the FCM converter

The instantaneous model of the 4-cell-5-level FCM (Fig. 2) converter in the state space representation can be described by

$$\begin{cases} \boldsymbol{X}'(t) = \boldsymbol{A}(\boldsymbol{S}(t))\boldsymbol{X}(t) + \boldsymbol{B}(\boldsymbol{S}(t))E \\ \qquad = \boldsymbol{f}(\boldsymbol{X}(t), \boldsymbol{S}(t)), \\ Y(t) = \boldsymbol{C}\boldsymbol{X}(t), \end{cases} \tag{3}$$

$$\boldsymbol{X}(t) = \begin{bmatrix} E_{\text{C1}}(t) & E_{\text{C2}}(t) & E_{\text{C3}}(t) & i_{\text{L}}(t) \end{bmatrix}^{\text{T}}, \tag{4}$$

$$\boldsymbol{A}(\boldsymbol{S}(t)) = \begin{bmatrix} 0 & 0 & 0 & (S_2 - S_1)/C_1 \\ 0 & 0 & 0 & (S_3 - S_2)/C_2 \\ 0 & 0 & 0 & (S_4 - S_3)/C_3 \\ \dfrac{S_1 - S_2}{L} & \dfrac{S_2 - S_3}{L} & \dfrac{S_3 - S_4}{L} & -\dfrac{R}{L} \end{bmatrix}, \tag{5}$$

$$\boldsymbol{B}(\boldsymbol{S}(t)) = \begin{bmatrix} 0 & 0 & 0 & (S_4 - 0.5)/L \end{bmatrix}^{\text{T}}, \tag{6}$$

$$\boldsymbol{C} = [0 \quad 0 \quad 0 \quad 1], \tag{7}$$

where E is the voltage of the input dc source, $\boldsymbol{S}=[S_1\ S_2\ S_3\ S_4]$ are the states of the switches, and $Y(t)=i_{\text{L}}(t)$ is the measured state and corresponds to the load current.

The main idea of the proposed strategy for estimating the flying capacitor voltages is based on the step-by-step calculation of state variables in each time interval using an approximated discrete model of the converter, which is written as follows:

$$\boldsymbol{X}'(t) = \boldsymbol{f}(\boldsymbol{X}(t), \boldsymbol{S}(t)). \tag{8}$$

Therefore,

$$\boldsymbol{X}(t + \Delta t) \approx \boldsymbol{X}(t) + \boldsymbol{f}(\boldsymbol{X}(t), \boldsymbol{S}(t)) \cdot \Delta t, \tag{9}$$

$$\boldsymbol{X}([k+1]\Delta t) \approx \boldsymbol{X}(k\Delta t) + \boldsymbol{f}(\boldsymbol{X}(k\Delta t), \boldsymbol{S}(k\Delta t)) \cdot \Delta t, \tag{10}$$

$$\boldsymbol{X}(k+1) \approx \boldsymbol{X}(k) + \boldsymbol{f}(\boldsymbol{X}(k), \boldsymbol{S}(k)) \cdot T, \tag{11}$$

where T is the sampling period, and it is reasonable to neglect T^2, T^3, ... For example, in the first time interval $kT<t<(k+1)T$ with known values of $\boldsymbol{X}(k)$ and $\boldsymbol{S}(k)$, we can calculate the value of $\boldsymbol{X}(k+1)$ at the end of the corresponding time interval; by substituting Eqs. (4)–(6) into Eq. (11), we have

$$\boldsymbol{X}(k+1) \approx \boldsymbol{X}(k) + T(\boldsymbol{A}(\boldsymbol{S}(k))\boldsymbol{X}(k) + \boldsymbol{B}(\boldsymbol{S}(k))E), \tag{12}$$

$$\boldsymbol{X}(k+1) \approx (1 + T\boldsymbol{A}(\boldsymbol{S}(k)))\boldsymbol{X}(k) + T\boldsymbol{B}(\boldsymbol{S}(k))E. \tag{13}$$

Using Eq. (13) makes it possible to estimate the flying capacitor voltages of the FCM converter step by step. By estimating the flying capacitor voltages, it is feasible to estimate the output voltage as follows:

$$\begin{aligned} V_{\text{out}}(t) = (S_4 - 0.5)E + (S_3 - S_4)E_{\text{C3}}(t) \\ + (S_2 - S_3)E_{\text{C2}}(t) + (S_1 - S_2)E_{\text{C1}}(t). \end{aligned} \tag{14}$$

The estimation strategy of the 4-cell FCM converter is shown in Fig. 5.

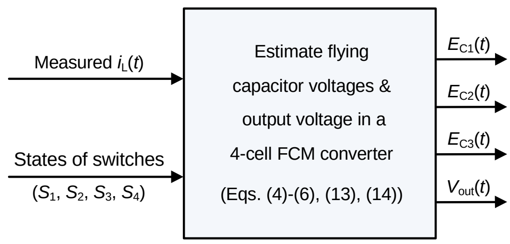

Fig. 5 Estimation strategy of the 4-cell-5-level flying capacitor multicell converter

4.2 Modeling of the SM converter

In the same way, it is possible to apply the similar equations to the SM converter. Therefore, the instantaneous model of the 4-cell-5-level SM converter (Fig. 4) in the state space representation can be described by

$$\begin{cases} \boldsymbol{X}'(t) = \boldsymbol{A}(\boldsymbol{S}(t))\boldsymbol{X}(t) + \boldsymbol{B}(\boldsymbol{S}(t))E \\ \quad = \boldsymbol{f}(\boldsymbol{X}(t), \boldsymbol{S}(t)), \\ Y(t) = \boldsymbol{C}\boldsymbol{X}(t), \end{cases} \tag{15}$$

$$\boldsymbol{X}(t) = \begin{bmatrix} E_{\mathrm{CP1}}(t) & E_{\mathrm{CP2}}(t) & i_{\mathrm{L}}(t) \end{bmatrix}^{\mathrm{T}}, \tag{16}$$

$$\boldsymbol{A}(\boldsymbol{S}(t)) = \begin{bmatrix} 0 & 0 & \frac{S_{\mathrm{P2}} - S_{\mathrm{P1}}}{C_{\mathrm{P1}}} \\ 0 & 0 & \frac{S_{\mathrm{N2}} - S_{\mathrm{N1}}}{C_{\mathrm{N1}}} \\ \frac{S_{\mathrm{P1}} - S_{\mathrm{P2}}}{L} & \frac{S_{\mathrm{N1}} - S_{\mathrm{N2}}}{L} & -\frac{R}{L} \end{bmatrix}, \tag{17}$$

$$\boldsymbol{B}(\boldsymbol{S}(t)) = \begin{bmatrix} 0 & 0 & (S_{\mathrm{P2}} + S_{\mathrm{N2}} - 1)/(2L) \end{bmatrix}^{\mathrm{T}}, \tag{18}$$

$$\boldsymbol{C} = [0 \quad 0 \quad 1], \tag{19}$$

where E is the voltage of the input dc source, $\boldsymbol{S} = [S_{\mathrm{P1}} \; S_{\mathrm{P2}} \; S_{\mathrm{N1}} \; S_{\mathrm{N2}}]$ are the states of switches, and $Y(t)=i_{\mathrm{L}}(t)$ is the measured state and corresponds to the load current.

By substituting Eqs. (16)–(18) into Eq. (13), it is possible to estimate the flying capacitor voltages in the 4-cell SM converter. Like in the FCM converter, it is feasible to estimate the output voltage using the estimated value of the flying capacitor voltages:

$$\begin{aligned} V_{\mathrm{out}}(t) = {} & (S_{\mathrm{P2}} + S_{\mathrm{N2}} - 1)E/2 + (S_{\mathrm{P1}} - S_{\mathrm{P2}})E_{\mathrm{CP1}}(t) \\ & + (S_{\mathrm{N1}} - S_{\mathrm{N2}}) \cdot E_{\mathrm{CN1}}(t). \end{aligned} \tag{20}$$

The estimation strategy of the 4-cell-5-level SM converter is shown in Fig. 6.

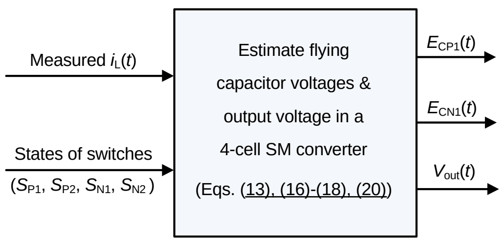

Fig. 6 Estimation strategy of the 4-cell-5-level stacked multicell converter

5 Simulation results

Computer simulation was performed to verify the effectiveness and behavior of the proposed estimation strategy in observing the flying capacitor voltages. The 4-cell-5-level FCM and SM converters were simulated using the PSCAD/EMTDC software. The main parameters used in the simulation are shown in Table 3.

Table 3 Main parameters of simulated circuit

System parameter	Value
DC voltage, E	200 V
Internal flying capacitors, C	1 mF
PS-SPWM carrier frequency	2100 Hz
Fundamental output voltage frequency	50 Hz
Load impedance, R_{L}, L_{L}	20 Ω, 50 mH
Sampling period, T	2 μs

5.1 Estimation of flying capacitor voltages in the FCM converter

In this case, input voltage E was 200 V at startup of the simulation and it was changed to 300 V at t=0.25 s after balancing the flying capacitors at their target values. Figs. 7–9 show the estimated voltage of the flying capacitors as well as the estimation errors of $E_{\mathrm{C1}}(t)$, $E_{\mathrm{C2}}(t)$, and $E_{\mathrm{C3}}(t)$, respectively. As shown in these figures, the proposed strategy can estimate the flying capacitor voltages precisely while the estimation errors were almost zero.

As shown in Fig. 10, estimating the flying capacitor voltages, knowledge of the switch states and using Eq. (14) make it possible to estimate the output voltage in the FCM converter.

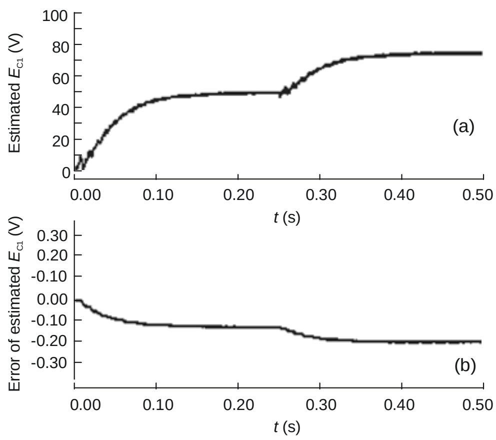

Fig. 7 Estimated voltage of cell-1's flying capacitor (a) and the estimation error (b) of the flying capacitor multicell converter

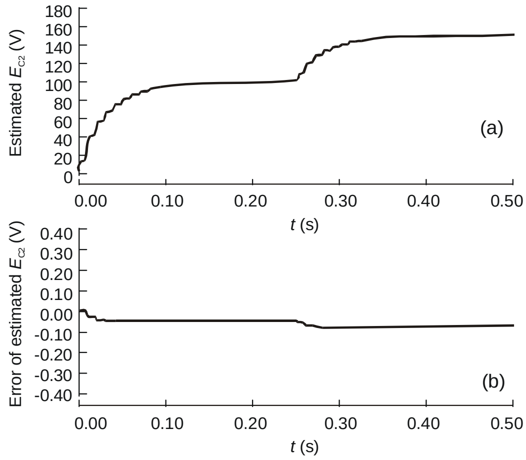

Fig. 8 Estimated voltage of cell-2's flying capacitor (a) and the estimation error (b) of the flying capacitor multicell converter

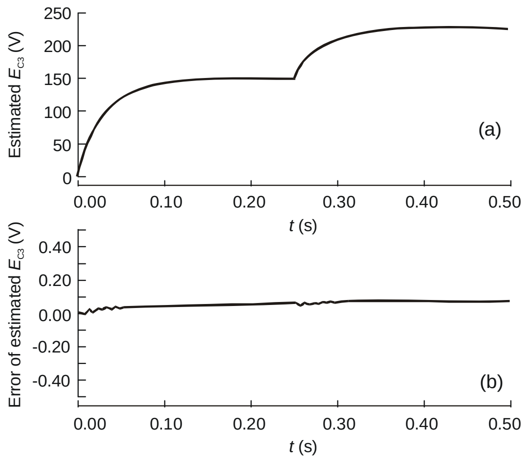

Fig. 9 Estimated voltage of cell-3's flying capacitor (a) and the estimation error (b) of the flying capacitor multicell converter

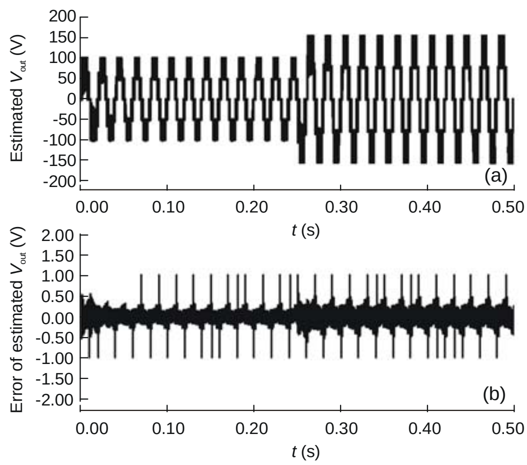

Fig. 10 Estimated output voltage (a) and the estimation error (b) of the flying capacitor multicell converter

5.2 Estimation of flying capacitor voltages in the SM converter

In this case, input voltage E was 200 V at startup of the simulation and it was changed to 300 V at t=0.25 s after balancing the flying capacitors at their target values. Figs. 11 and 12 show the estimated voltage of flying capacitors as well as the estimation errors of $E_{CP1}(t)$ and $E_{CN1}(t)$, respectively. As shown in these figures, the proposed strategy can estimate the flying capacitor voltages precisely while the estimation errors were almost zero.

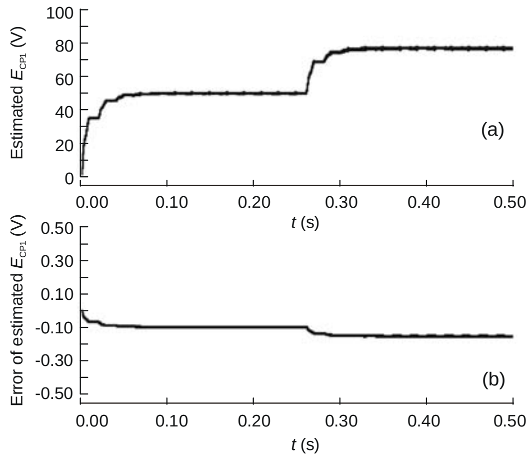

Fig. 11 Estimated voltage of cell-P1's flying capacitor (a) and the estimation error (b) of the stacked multicell converter

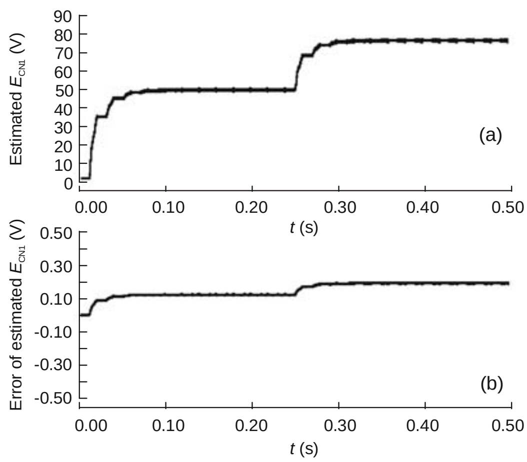

Fig. 12 Estimated voltage of cell-N1's flying capacitor (a) and the estimation error (b) of the stacked multicell converter

As shown in Fig. 13, estimating the flying capacitor voltages, knowledge of the switches states and using Eq. (20) make it possible to estimate the output voltage in the SM converter.

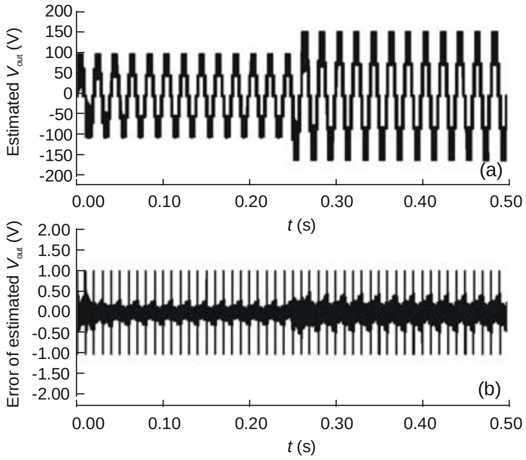

Fig. 13 Estimated output voltage (a) and the estimation error (b) of the stacked multicell converter

6 Conclusions

To take full advantage of FCM and SM converters, the flying capacitor voltages must be balanced to their optimal and desired values. Moreover, it is essential to know the flying capacitor voltages in the active control technique. Using differential voltage sensors for measuring the flying capacitor voltages, however, results in an increase in the drive cost and size.

To reduce the number of sensors in these converters and, consequently, the cost of the control system, we modeled the converter in the state space representation and proposed a simple estimation strategy based on a discrete time model of the converter using only the load current sensors. The proposed strategy is simple and precise. Simulation results showed that the proposed estimation strategy can be used to observe the flying capacitor voltages and the output voltage with almost zero estimation errors.

References

Babaei, E., Hosseini, S.H., Gharehpetian, G.B., Tarafdar Haque, M., Sabahi, M., 2007. Reduction of dc voltage sources and switches in asymmetrical multilevel converters using a novel topology. *J. Electr. Power Syst. Res.*, **77**(8):1073-1085. [doi:10.1016/j.epsr.2006.09.012]

Haederli, C., Ladoux, P., Meynard, T., Gateau, G., Lienhardt, A.M., 2006. Neutral Point Control in Multilevel Converters Applying Novel Modulation Schemes. IEEE 37th Power Electronics Specialists Conf., p.1-8. [doi:10.1109/PESC.2006.1711981]

Halvaei Niasar, A., Vahidi, A., Moghbell, H., 2009. Low-cost sensorless control of four-switch, brushless DC motor drive with direct back-EMF detection. *J. Zhejiang Univ. Sci. A*, **10**(2):201-208. [doi:10.1631/jzus.A0820097]

Hosseini, S.H., Khoshkbar Sadigh, A., Sharifi, A., 2009. Estimation of flying capacitors voltages in multicell converters. 6th Int. Conf. on Electrical Engineering/ Electronics Computer Telecommunications and Information Technology, p.110-113. [doi:10.1109/ECTICON.2009.5136976]

Hu, J.B., He, Y.K., 2007. Multi-frequency proportional-resonant (MFPR) current controller for PWM VSC under unbalanced supply conditions. *J. Zhejiang Univ. Sci. A*, **8**(10):1527-1531. [doi:10.1631/jzus.2007.A1527]

Hu, J.B., He, Y.K., Heng, N., 2007. Enhanced control of DFIG-used back-to-back PWM VSC under unbalanced grid voltage conditions. *J. Zhejiang Univ. Sci. A*, **8**(8):1330-1339. [doi:10.1631/jzus.2007.A1330]

Khoshkbar Sadigh, A., Babaei, E., Hosseini, S.H., Farasat, M., 2009a. Dynamic Voltage Restorer Based on Stacked Multicell Converter. IEEE Symp. on Industrial Electronics and Application, p.419-424. [doi:10.1109/ISIEA.2009.5356441]

Khoshkbar Sadigh, A., Hosseini, S.H., Barakati, S.M., Gharehpetian, G.B., 2009b. Flying Capacitor Multicell Converter Based Dynamic Voltage Restorer. 41st North American Power Symp., p.1-6. [doi:10.1109/NAPS.2009.5484074]

Khoshkbar Sadigh, A., Hosseini, S.H., Barakati, S.M., Gharehpetian, G.B., 2009c. Stacked Multicell Converter Based DVR with Energy Minimized Compensation Strategy. 41st North American Power Symp., p.1-6. [doi:10. 1109/NAPS.2009.5484075]

Lezana, P., Silva, C.A., Rodríguez, J., Pérez, M.A., 2007. Zero steady state error input-current controller for regenerative multilevel converters based on single-phase cells. *IEEE Trans. Ind. Electron.*, **54**(2):733-740. [doi:10.1109/TIE.2007.891994]

Lezana, P., Rodríguez, J., Oyarzún, D.A., 2008a. Cascaded multilevel inverter with regeneration capability and reduced number of switches. *IEEE Trans. Ind. Electron.*, **55**(3):1059-1066. [doi:10.1109/TIE.2008.917095]

Lezana, P., Ortiz, G., Rodríguez, J., 2008b. Operation of Regenerative Cascade Multicell Converter under Fault Condition. 11th Workshop on Control and Modeling for Power Electronics, p.1-6. [doi:10.1109/COMPEL.2008.4634667]

Li, C.H., Zhu, X.J., Cao, G.Y., Hu, W.Q., Sui, S., Hu, M.R., 2009. A maximum power point tracker for photovoltaic energy systems based on fuzzy neural networks. *J. Zhejiang Univ. Sci. A*, **10**(2):263-270. [doi:10.1631/jzus.A0820128]

Lienhardt, A.M., Gateau, G., Meynard, T.A., 2006a. Stacked Multicell Converter: Digital Sliding Mode Observation of Flying Capacitor Voltages. 32nd Annual Conf. on IEEE

Industrial Electronics, p.2115-2120. [doi:10.1109/IECON.2006.347799]

Lienhardt, A.M., Gateau, G., Meynard, T.A., 2006b. Stacked Multicell Converter: Sliding Mode Observation of Flying Capacitor Voltages. IEEE Int. Symp. on Industrial Electronics, p.970-976. [doi:10.1109/ISIE.2006.295767]

Lienhardt, A.M., Gateau, G., Meynard, T.A., 2007. Digital sliding-mode observer implementation using FPGA. *IEEE Trans. Ind. Electron.*, **54**(4):1865-1875. [doi:10.1109/TIE.2007.898305]

Ma, M.Y., He, X.N., 2008. Synchronization analysis on cascaded multilevel converters with distributed control. *J. Zhejiang Univ. Sci. A*, **9**(2):190-198. [doi:10.1631/jzus.A071319]

McGrath, B.P., Holmes, D.G., 2008. Natural current balancing of multicell current source converters. *IEEE Trans. Power Electron.*, **23**(3):1239-1246. [doi:10.1109/TPEL.2008.921166]

McGrath, B.P., Meynard, T.A., Gateau, G., Holmes, D.G., 2007. Optimal modulation of flying capacitor and stacked multicell converters using a state machine decoder. *IEEE Trans. Power Electron.*, **22**(2):508-516. [doi:10.1109/TPEL.2006.889932]

Meynard, T.A., Fadel, M., Aouda, N., 1997. Modeling of multilevel converters. *IEEE Trans. Ind. Electron.*, **44**(3):356-364. [doi:10.1109/41.585833]

Meynard, T.A., Foch, H., Forest, F., Turpin, C., Richardeau, F., Delmas, L., Gateau, G., Lefeuvre, E., 2002. Multicell converters: derived topologies. *IEEE Trans. Ind. Electron.*, **49**(5):978-987. [doi:10.1109/TIE.2002.803189]

Meynard, T.A., Lienhardt, A.M., Gateau, G., Haederli, C.H., Barbosa, P., 2006. Flying Capacitor Multicell Converters with Reduced Stored Energy. IEEE Symp. on Industrial Electronics, p.1-5.

Nabae, A., Takahashi, I., Akagi, H., 1981. A new neutral point clamped PWM inverter. *IEEE Trans. Ind. Appl.*, **17**(5):518-523. [doi:10.1109/TIA.1981.4503992]

Ruelland, R., Gateau, G., Meynard, T.A., Hapiot, J.C., 2003. Design of FPGA-based emulator for series multicell converters using co-simulation tools. *IEEE Trans. Power Electron.*, **18**(1):455-463. [doi:10.1109/TPEL.2002.807104]

Sayyah, A., Aflaki, M., Rezazadeh, A., 2008. Optimization of total harmonic current distortion and torque pulsation reduction in high-power induction motors using genetic algorithms. *J. Zhejiang Univ. Sci. A*, **9**(12):1741-1752. [doi:10.1631/jzus.A0820055]

Turpin, C., Deprez, L., Forest, F., Richardeau, F., Meynard, T.A., 2002. A ZVS imbricated cell multilevel inverter with auxiliary resonant commutated poles. *IEEE Trans. Power Electron.*, **17**(6):874-882. [doi:10.1109/TPEL.2002.805593]

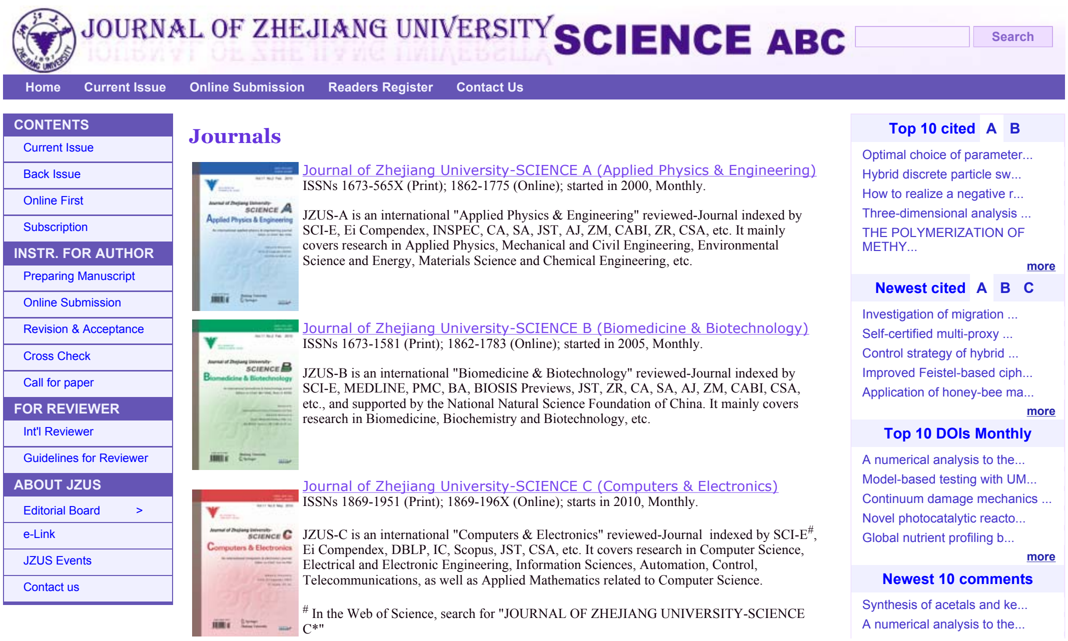

Journals of Zhejiang University-SCIENCE (A/B/C) **website, http://www.zju.edu.cn/jzus**

When an article is commented by a reader, or cited by an ISI journal or proceeding, an e-mail notification will be sent automatically to the author(s). For each article, statistics such as downloads, clicks, citations, and comments are given in the contents of each issue